The 6th International Conference on
Structural Health Monitoring of Intelligent Infrastructure
Hong Kong | 9-11 December 2013

BRIDGE LOCAL SCOUR MONITORING USING SMART ROCK

S. H. Jiang, Z. Zhou and J. P. Ou
School of Civil Engineering, Dalian University of Technology, Dalian 116024, China
E-mail: jiangsh@whu.edu.cn; zhouzhi@dlut.edu.cn; oujinping@dlut.edu.cn

ABSTRACT

The bridge local scour monitoring is characterized as harsh service environment, extensive arranged sensors, etc. So the monitoring method using smart rock is raised as a dynamic scour sensor in the paper. The bridge local scour monitoring system consists of smart rock and magnetic gradiometer. The magnetic label is casted into concrete to construct smart rock, which can be three dimensionally localized by means of magnetic survey. The dynamic scour performance is studied on the basis of simplification of vortex and force of smart rock. The bottom velocity at the front of bridge pier is analyzed based on the existing scour mechanism; the loading characteristic and moving mode of smart rock is analyzed by means of Hertz contact theory. The relationship between diameter of smart rock and approach velocity is studied for dynamic scour monitoring method. The result shows when the approach velocity is smaller than 7m/s, the smart rock can be effectively used for scour monitoring, with the diameter of 0.5 m.

KEYWORDS

Bridge, smart rock, magnetic survey, local scour, monitoring.

INTRODUCTION

Bridge scour is one of the main causes of bridge failures. There are approximately 600,000 bridges in the United States and 500,000 of them are over water (Gee 2003). During the past 30 years, more than 1,000 of the 500,000 bridges have failed, with 60% of those failures related to bridge scour, with overload and earthquakes accounting for only 10% and 2% respectively (Shirole and Holt 1991). Bridge scour has been proven to be the most common cause of highway bridge failures in the United States (Lagasse *et al.* 2001). Furthermore, the bridge failure due to scour occurs in the water, which is characterized as concealment without obvious sign, difficult and expensive to repair. The cost for scour-related bridge failures was estimated at $30 million per year (Lagasse *et al.* 1997), and bridge scour maintenance costs comprises more than 70% of total expenditure for bridge transportation (Melville 1992). Therefore, it's essential to monitor the bridge scour through the whole process of service.

At present, there are many existing methods for bridge scour detection and monitoring, such as sonar (Deng *et al.* 2010), radar (Hayden *et al.* 2011), Time Domain Reflectometry (TDR) (Yu *et al.* 2011), optical fiber (Zhou *et al.* 2011), sliding collar, dropping weights, buoyancy "fish" (Yankielun and Zabilansky 1999), Radio Frequency Identification (RFID) (Lauth and Papanicolaou 2008), Micro-Electro-Mechanical Systems (MEMS) (Lin *et al.* 2010), etc. Despite the critical need for a real-time scour monitoring system, the harsh environment has prevented the advancement of a real-time scour monitoring system. Since river bed, especially around the structure, fluctuates due to rapid and intensive scour during high water flood conditions and rapid water movements that cause muddy water mixtures, safe, rugged and online measurement of scour situation has always been very difficult. The present monitoring technologies, not sufficiently rugged enough, are mostly taken after flood events. On the other hand, the safety of bridge pier is strongly related to the local sour state. So it is necessary to develop the real time monitoring for local scour in the harsh environment. A durable and robust system capable of providing real time continuous monitoring of scour in various environmental conditions is needed to advance the current state of practice.

In the paper, the conception of smart rock, dynamic scour sensor, is developed on the basis of the magnetic localization. In order to study the dynamic scour characteristic, the water stream velocity at front of bridge pier is simplified, and the force of smart rock is analyzed to realize the dynamic scour monitoring using Hertz contact theory. The smart rock can also be used for riprap, which is verified to be practical in comparison with

other experimental formula.

BRIDGE LOCAL SCOUR MONITORING SYSTEM

The bridge local scour monitoring system is composed of smart rock and magnetic gradiometer, see Figure 1. The magnetic label is encapsulated in the concrete as smart rock, and the magnetic gradiometer is installed at the front of bridge pier. When the bridge scour occur and develop, the smart rock will move with the evolution of scour hole. According to the localization by magnetic gradiometer, the three dimensional displacement of smart rock can be obtained to reflect the bridge local scour depth.

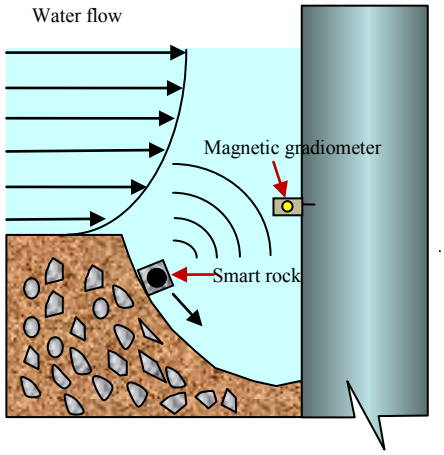

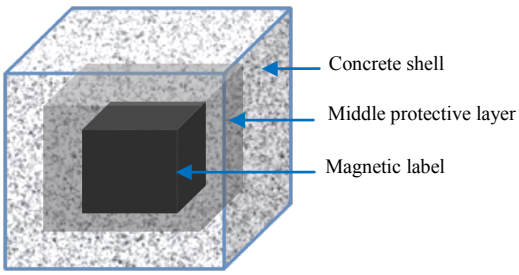

Figure 1. Bridge local scour monitoring system

Figure 2. Formation of smart rock

The smart rock is composed of magnetic label, middle protective layer and concrete shell, see Figure 2. The middle protective layer includes rubber and engineering plastic that are used for anti- shock and anti- seepage respectively. To resist the chemical erosion and physical abrasion in the complex fluid condition, the magnetic label packaged in the middle protective layer is casted in the concrete, i.e. smart rock. The magnetic label is a Nd-Fe-B magnet placed in the center of a gimbal.

LOCALIZATION OF SMART ROCK USING MAGNETIC GRADITENT TENSOR

Since the Earth's magnetic field B_E (50,000nT) is orders of magnitude larger than magnetic anomaly fields B_A (1nT) (Filipski and Abdulah 2006), direct measurements of B_A from a total field $B_T = B_E + B_A$ is very complicated. Recently, some researchers use the gradiometer sensor system to reduce the effects of B_E. Moreover, the gradient of B_E, $\nabla B_E \approx 0.02$nT/m (Merlat and Naz 2003), is much less than that of B_A, so that $\nabla B_T = \nabla B_E + \nabla B_A \approx \nabla B_A$. The localization of magnetic objects can be realized by magnetic gradient tensor.

The smart rock can be regarded as a magnetic dipole, and the vector magnetic field $\boldsymbol{B}$ at a distance $\boldsymbol{r}$ can be calculated as

$$\boldsymbol{B} = \frac{\mu_0}{4\pi}\left[\frac{3(\boldsymbol{m}\bullet\boldsymbol{r})\boldsymbol{r}}{r^5} - \frac{\boldsymbol{m}}{r^3}\right] \tag{1}$$

Where, $\mu_0 = 4\pi \times 10^{-7}$ Tm/A is the magnetic permeability, and $\boldsymbol{m}$ is magnetic moment of smart rock.

And the magnetic gradient of smart rock is a tensor whose matrix elements is given by (Wynn 1995)

$$\boldsymbol{G}_{ij} = \frac{\partial B_i}{\partial r_j} = \frac{\mu_0}{4\pi}\left[-\frac{15(\boldsymbol{m}\bullet\boldsymbol{r})r_i r_j}{r^7} + \frac{\boldsymbol{3}m_i r_j}{r^5} + \frac{\boldsymbol{3}m_j r_i}{r^5} + \frac{3(\boldsymbol{m}\bullet\boldsymbol{r})\delta_{ij}}{r^5}\right] \tag{2}$$

$$\delta_{ij} = \begin{cases} 1 & i = j \\ 0 & i \neq j \end{cases} \tag{3}$$

The magnetic gradient tensor $\boldsymbol{G}$ can be expressed in terms of spatial derivatives in Cartesian components (x, y, z), generating 9 components, i.e. B_{xx}, B_{xy}, B_{xz}, B_{yx}, B_{yy}, B_{yz}, B_{zx}, B_{zy}, B_{zz}. In a region free of distributed currents, the magnetic field satisfies $\nabla\times\boldsymbol{B}=0$, and this means that $\boldsymbol{G}$ is symmetric, i.e. $B_{xy}-B_{yx}=0$, $B_{xz}-B_{zx}=0$, $B_{yz}-B_{zy}=0$. At the same time, $\nabla\bullet\boldsymbol{B}=0$, and the matrix $\boldsymbol{G}$ is tracelss, i.e. $\text{trace}\boldsymbol{G}=B_{xx}+B_{yy}+B_{zz}=0$. Consequently, $\boldsymbol{G}$ has only 5 independent components, B_{xx}, B_{xy}, B_{xz}, B_{yy}, B_{yz}.

When the smart rock moves, it's assumed that azimuth angle is (θ,φ) for Nd-Fe-B magnet, θ = the angle between the dipole axis and Z axis, φ = the angle between the dipole axis and X axis. There are location parameters $\boldsymbol{r}$ (x, y, z) and moment parameters $\boldsymbol{m}$($m\sin\theta\cos\varphi$, $m\sin\theta\sin\varphi$, $m\cos\theta$), i.e. $\boldsymbol{m}$(m_x, m_y, m_z) for Nd-Fe-B magnet. So there is 5 freedoms for Nd-Fe-B magnet, i.e. (x, y, z, θ, φ).

The Nd-Fe-B magnet is placed in the center of the gimbal in order that the dipole axis keeps vertical, i.e. $\theta = 0$, when the smart rock rolls, tilts or rotates. The moment parameters $\boldsymbol{m}$(m_x, m_y, m_z) is simplified to $\boldsymbol{m}$(0, 0, m) to eliminate the rotational degree of freedom (θ, φ). In this way, the motion of Nd-Fe-B magnet is reduced to 3 translational degrees of freedom $\boldsymbol{r}$ (x, y, z).

In the practical measurement system, the magnetic gradient tensor is obtained by the assembly of several magnetic probes. So the magnetic gradient tensor of smart rock is given by

$$\mathrm{G}_{ij} = \frac{\partial B_i}{\partial r_j} \approx \frac{\Delta B_i}{\Delta l} = \frac{\sum_{k=1}^{n}\left(B_{i2}-B_{i1}\right)}{nd} \tag{4}$$

Where, d is the baseline of magnetic probes; n is the number of magnetic probes along each axis. $\Delta B_i/\Delta l$ is the magnetic gradient tensor measured by magnetic gradiometer, i.e. $\Delta B_x/\Delta x$, $\Delta B_x/\Delta y$, $\Delta B_x/\Delta z$, $\Delta B_y/\Delta y$, $\Delta B_y/\Delta z$; $\partial B_i/\partial r_j$ is the magnetic gradient tensor calculated by above mentioned equations, i.e. B_{xx}, B_{xy}, B_{xz}, B_{yy}, B_{yz}, everyone of which has the unknown parameters $\boldsymbol{r}(x,y,z)$.

The unknown parameters of Eq. 4 is reduced from (x, y, z, θ, φ) to $\boldsymbol{r}$ (x, y, z) by means of gyroscope. The nonlinearity of equation set is lessen so that it can be resolved by the optimizing search to get the position vector $\boldsymbol{r}$ (x, y, z) (Jiang *et al.* 2012).

To the target with magnetic moment of 15 A.m^2 and the magnetic sensor with the precision of 0.2 nT, the maximum detection distance by magnetic gradiometer can reach 12 m with localization error of 0.3 m (Ren and Hua 2010). In this paper, by means of the magnetic gradiometer with the precision of 0.002 nT, the maximum detection distance can exceed 20 m (Jiang *et al.* 2013b).

SIMPLIFICATION OF HORSESHOE VORTEX AT FRONT OF BRIDGE PIER

Bridge local scour is mainly caused by the horseshoe vortex around the bridge. As the stream flow approaches the pier, an adverse pressure gradient due to the pier drives a portion of the approach flow downward just ahead of the pier, and then the down flow forms the vortex on the level of riverbed in the front of pier. At the same time, the vortex rotates at the nose of the pier and passes along the sides of the pier in the downstream direction. Erosion occurs when the shear stress because of the vortex acting on the sediment surface exceeds the critical value. Hence, the bottom velocity of vortex is the basis for the bridge scour monitoring and protection.

With regard to the vortex in the front of pier, the radial velocity (r) is much larger than tangential velocity (θ) or vertical velocity (z) (Subhasish and Rajkumar 2007), see Figure 3. So it can be assumed that the sediment erosion is led by the radial flow of vortex in front of the pier, and the three dimensional vortex is simplified to the two dimensional vortex, see Figure 4.

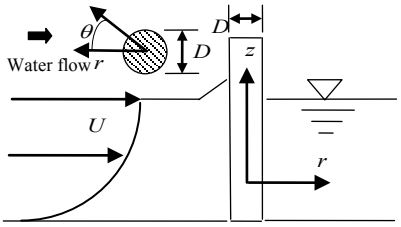

Figure 3. Coordinate for bridge local velocity

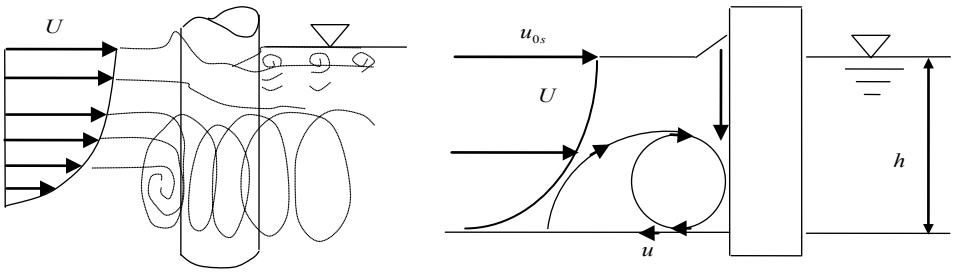

(a) the horseshoe vortex (b) Simplified vortex

Figure 4. Sketch of velocity at front of bridge pier

Due to the presence of the pier, the local circulation of the approach flow is decreased at front of the pier. Assuming no slip on the solid boundaries and using ideal fluid theory, the decrease of local circulation could be presented as (Shen *et al.* 1969)

$$\Gamma_1 = -0.5u_{0s}D \tag{5}$$

Where u_{0s} is the surface velocity of the approach flow, and D is the diameter of the pier.

The circulation of vortex in the Figure 4 (b) can be given by

$$\Gamma_2 = -2\pi au \tag{6}$$

Where, u is the tangential velocity at the circumference of the vortex and is assumed to be acting at the particle level; a is the radius of rotation of the vortex, which is assumed to be $0.177D$ regardless of pier Reynolds number.

It's assumed that the two circulations Γ_1 and Γ_2, are equated (Nagagawa and Suzuki 1975), and the bottom velocity can be expressed as

$$u = 0.450u_{0s} \tag{7}$$

The vertical flow velocity distribution is described as

$$u = U\left(1+1/n\right)\left(y/n\right)^{\frac{1}{n}} \tag{8}$$

Where, n is the constant related to the riverbed feature usually ranged from 5 to 9 (value of 6 is used for n in this study); U is the approach velocity.

By the combination of Eqs 7 and 8, the bottom velocity at front of bridge pier can be given as

$$u = 0.525U \tag{9}$$

The maximum of bottom velocity u, occurs at some depth beneath at the level of the original bed elevation. From this depth to the bottom of the scour hole, the velocity gradually decrease (Johnson and McCuen 1991). In terms of the motion and force analysis for the smart rock, the bottom velocity in the scour hole is approximately assumed to be that at the level of original bed elevation.

BRIDGES LOCAL SCOUR DEPETH MONITORING USING SMART ROCK

The shape of scour hole can be approximated to a frustum of an inverted cone with an angle of frustum equal to the angle of repose of bed sediment. The scour hole in front of pier can be simplified as the two dimensional slope, and the evolution of scour hole can be regarded as the expansion of slope. Accordingly, the smart rock

moves as the development of scour hole, see Figure 5.

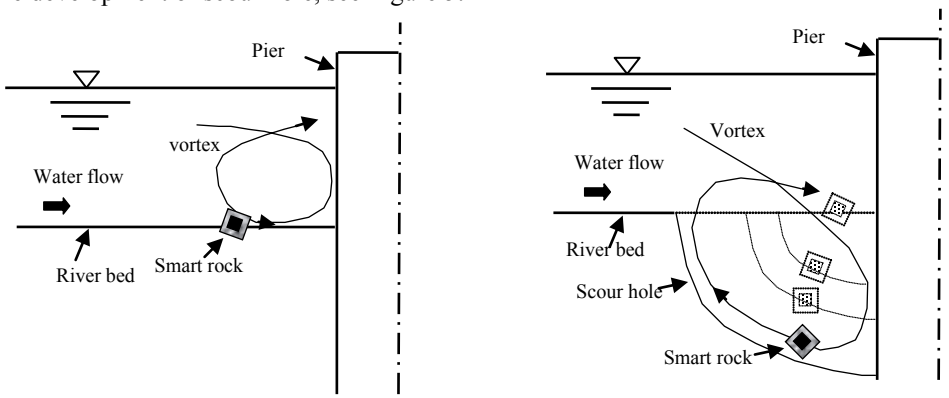

(a) Before scour (b) Scour hole and the move of smart rock

Figure 5. Scour monitoring of smart rock

The main forces acting on the smart rock are submerged weight W, hydrodynamic drag force F_D, and hydrodynamic lift force F_L, as shown in Figure 6. The smart rock is approximated to a spherical rock with the diameter of d. The expressions for the forces are given by

$$W = (\gamma_s - \gamma)\frac{\pi d^3}{6} \tag{10}$$

$$F_D = \gamma C_D \frac{\pi d^2}{4}\frac{u^2}{2g} \tag{11}$$

$$F_L = \gamma C_L \frac{\pi d^2}{4}\frac{u^2}{2g} \tag{12}$$

Where, u is the bottom velocity of bed level; C_D and C_L are drag and lift coefficients respectively (C_D = 0.4 and C_L = 0.1 are used in this study); γ and γ_s are specific weigh of water and the smart rock respectively (γ = 1.0 kN/m^3 and γ_s = 2.6 kN/m^3 are used).

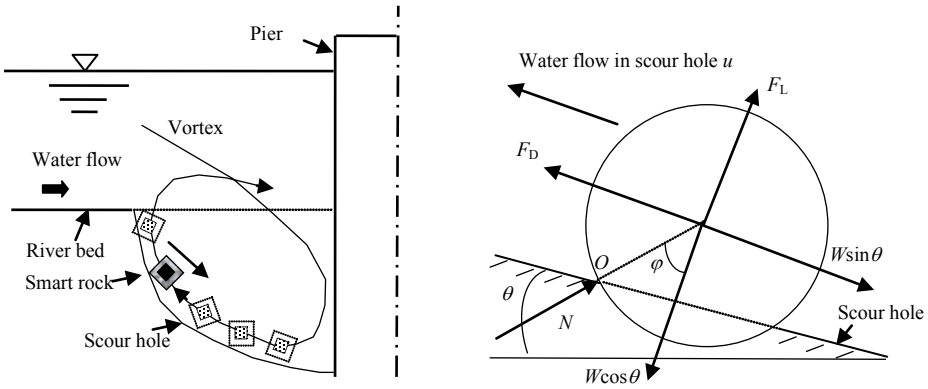

(a) Motion of smart rock in the scour hole (b) Simplification of forces acting on smart rock

Figure 6. Scheme of force for smart rock

Depending on the characteristics of a near-bed flow, a smart rock resting in the scour hole can move in either one of the following three modes, namely lifting, sliding or rolling, which can be expressed in the form

$$F_L < W\cos\theta \tag{13}$$

$$F_D - W\sin\theta < (W\cos\theta - F_L)f \tag{14a}$$

$$F_L + f^{-1}F_D < W(\cos\theta + f^{-1}\sin\theta) \tag{14b}$$

$$K_D(F_D - W\sin\theta) < K_L(W\cos\theta - F_L) \tag{15a}$$

$$K_D F_D + K_L F_L < W(K_D\sin\theta + K_L\cos\theta) \tag{15b}$$

Where, θ is slope angle of scour holing; $\theta = 32.5 + 1.27d_{50}$ is defined (d_{50} = diameter of sediment particle, $d_{50} \leqslant$ 2mm) (Zhou and Cui 1995), and value of 32.5 is used for θ in this study. f is coefficient of friction between smart rock and riverbed, and $f = \tan\phi$ is defined with ϕ angle of repose ranged from 30° to 40° (value of 35 is

used) (Zhang and Xu 2011). K_D and K_L are coefficients of moment arms corresponding to the drag force and lifting force respectively ($K_D = 0.5d\cos\varphi$ and $K_L = 0.5d\sin\varphi$ is assumed).

The smart rock resting on the riverbed can be seen as a rigid sphere with diameter of d, which contacts with a half space. According to the Hertz contact theory (Valentin 2011), the relationship between incipient yield normal load and incipient yield normal deformation can be given by

$$P_y = \frac{2\sqrt{2}}{3} E^* d^{\frac{1}{2}} \delta_y^{\frac{3}{2}} \quad (16)$$

Where, E^* is equivalent elastic modulus with the formulation of $E^* = E/(1-\nu^2)$ (E = 10Mpa is elastic modulus of riverbed sediment, $\nu = 0.33$ is poisson ratio of riverbed sediment); δ_y is incipient yield normal deformation.

The incipient yield normal deformation δ_y, can be expressed as

$$\delta_y = 0.125 d\pi^2 p_y^2 / E^* \quad (17)$$

Where, p_y is incipient yield stress with the definitions of $p_y = C_v Y$ and $C_v = 1.234+1.256\nu$ (Y is yield strength ranged from 5kPa to 50kPa, and value of 10kPa is used for Y in this study).

The relationship between normal load P and normal deformation δ can be given as

$$\delta = (P-P_y)/(\pi d p_y) + \delta_y \quad (18)$$

Where, δ is total normal deformation and $\delta = 0.5d(1-\cos\varphi)$ is used in this study; and $W\cos\theta$-F_L is valued for P.

Using Eqs from 10 to 15, the diameter of smart rock can be obtained

$$d > \frac{3\alpha\gamma u^2}{4g(\gamma_s - \gamma)} \quad (19)$$

Where, u calculated by Eq. 9, is the bottom velocity of bed level; α is motion mode coefficient of smart rock, and α is the maximum of α_1, α_2 and α_3. For lifting, $\alpha_1 = C_L/\cos\theta$; For sliding, $\alpha_2 = (C_L f + C_D)/(f\cos\theta + \sin\theta)$; For rolling, $\alpha_3 = (K_D C_D + K_L C_L)/(K_D\sin\theta + K_L\cos\theta)$.

The smart rock can be used as riprap for scour protection before bridge local scour, and accordingly, $\theta = 0$ is used for α in the computation for the smart rock.

CHARACTERISITIC ANALYSIS OF DYANAMIC SCOUR MONITORING USING SMART ROCK

The flow velocity is usually smaller than 3 m/s for rivers in plain region, while the maximum velocity can reach 5m/s for rivers in mountain region. Consequently, the approach velocity is supposed to ranged from 1 m/s to 7m/s. For scour monitoring, the relationship between diameter of smart rock and approach velocity is analyzed; when the smart rock is used as riprap for scour protection before local scour, i.e. $\theta = 0$, the relation between the diameter of smart rock and approach velocity can obtained, see Figure 7. The motion mode coefficient is also calculated, see Figure 8.

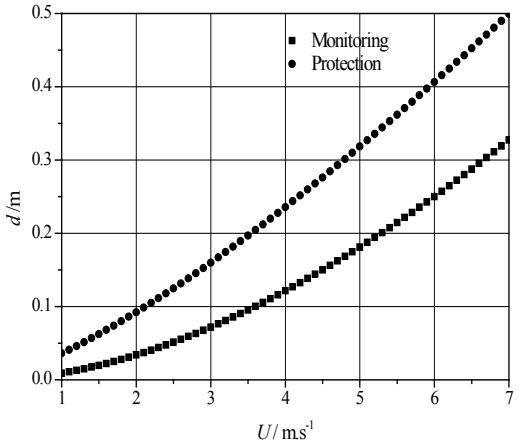

Figure 7. Relation between d and U

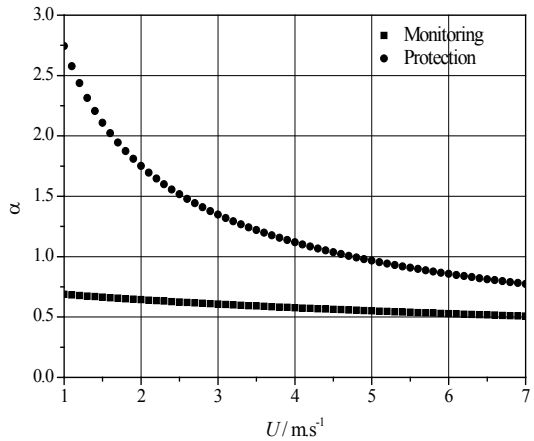

Figure 8. Relation between α and U

The Figure 7 indicates that the smart rock with the diameter of 0.33m (for approach velocity < 7m/s) can track

the scour hole to realize the monitoring of bridge local scour depth. The smart rock with the diameter of 0.50 m can be used as riprap. The weight of smart rock is about 170 kg with the diameter of 0.5 m, which is easy to fabrication and construction, and suitable for the scour monitoring during the flood.

From the Figure 8, it shows that in the scour hole the motion mode coefficient α is larger than α_1 (about 0.1186), and is larger than α_2 (about 0.4167); before scour, α is larger than α_1 (about 0.1), and is larger than α_2 (about 0.6713). So the motion mode of smart rock is rolling before and during the bridge scour.

According to the experiment research of pebble and rock, the formula of riprap initiation in front of bridge pier can be given as (Zhou *et al.* 1999; Jiang *et al.* 2013a)

$$d > \frac{0.139\gamma U^2}{g(\gamma_s - \gamma)} \tag{20}$$

When the smart rock is used for scour protection, the results from formula (19) and (20) are compared, see Figure 9.

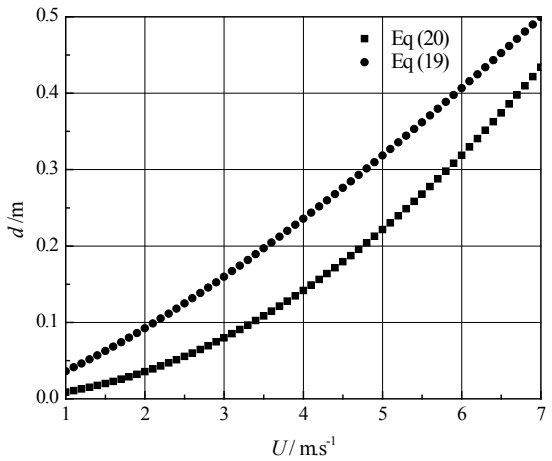

Figure 9. Comparison of theoretical Eq. 19 and experimental Eq. 20

From Figure 9, it shows that the diameter of smart rock from Hertz contact theory is slightly larger than that of the experimental formula when used as riprap before scour, and further more the smart rock can move in the scour hole to track the scour depth. So the smart rock can realize the bridge scour monitoring and protection.

CONCLUSIONS

Developing for real time scour monitoring under harsh flood conditions is a pressing task for the research community. In this study, the conception of smart rock is put forward for bridge local scour monitoring. The system consists smart rock and magnetic gradiometer, and the magnetic localization is used to monitor the three dimensional displacements of smart rock to realize the real time scour monitoring.

The smart rock can be conveniently thrown in front of the bridge, with no necessity of wires arrangement or maintenance, which is not influenced by the physical impact or chemical erosion of water flow, sediment and bridge, etc. The smart rock can be extensively arranged for long term service, which is apt for the scour monitoring during flood.

The dynamic monitoring feature is studied for the smart rock based on the simplification of vortex ahead of bridge pier and the shape of scour hole. By means of Hertz contact theory, the force and motion mode of smart rock is analyzed to obtain the relation between the diameter of smart rock in scour hole and approach flow. The results show that when the approach velocity is smaller than 7 m/s, the smart rock with the diameter of 0.5 m can dynamically monitor the scour depth in front of bridge, with the integration of scour protection.

In the paper, the smart rock is fabricated by the magnetic localization technology, and the conception of smart rock can be extended to ZigBee, Radio Frequency Identification and other localization technology that can penetrate the water flow and sediments.

ACKNOWLEDGEMENTS

The authors gratefully acknowledge the financial support from the Natural Science Foundation of China (No. 51208078).

REFERENCES

Deng, L. and Cai, C.S. (2010), "Bridge scour: prediction, modeling, monitoring, and countermeasures - review", *Practice periodical on structural design and construction*, 5, 125-134.

Filipski, M.N. and Abdulah, E.J. (2006). "Nanosatellite navigation with the WMM2005 geomagnetic field model", *Turkish Journal of Engineering & Environmental Sciences*, 30(1), 43-56.

Gee, K.W. (2003). "Action: compliance with the national bridge inspection standards—plan of action for scour critical bridges", *FHWA Bridge Technology Memorandum*.

Hayden, J.T. and Puleo, J.A. (2011). "Near real-time scour monitoring system: application to Indian River Inlet, Delaware", *Journal of hydraulic engineering*, 8, 1037-1046.

Jiang, S.H., Zhou, Z. and Ou, J.P. (2012). "Slope deformation monitoring principle based on magnetic gradient tensor", *Chinese Journal of Geotechnical Engineering*, 34 (10), 1944-1949 (in Chinese).

Jiang, S.H., Zhou, Z. and Ou, J.P. (2013a). "Initiation of rock motion for bridge local scour protection", *Journal of sediment research*, 8, 63-67 (in Chinese).

Jiang, S.H., Zhou, Z. and Ou, J.P. (2013b). "Slope internal large deformation monitoring using magnetic survey", *Rock and Soil Mechanics*, 2013, 34(10), in press, (in Chinese).

Johnson, P.A. and McCuen, R.H. (1991). *A Temporal Spatial Pier Scour Model*, Transportation Research Record, 1319, 143-149.

Lagasse, P.F., Richardson, E.V., Schall, J.D. and Price, G.R. (1997). *Instrumentation for Measuring Scour at Bridge Piers and Abutments*, Transportation Research Board, NCHRP Report 396, National Research Council, National Academy Press, Washington, DC.

Lagasse, P.F., Zevenbergen, L.W., Schall, J.D. and Clopper, P.E. (2001). "Bridge scour and stream instability countermeasures", *Hydraulic Engineering Circular 23*, Federal Highway Administration, Washington, D.C.

Lauth, T.J. and Papanicolaou, A.N. (2008). "Experimental/Feasibility Study of Radio Frequency Tracers for Monitoring Sediment Transport and Scour around Bridges", *Proceedings of the World Environmental and Water Resources Congress*, Ahupua'a, 345-354.

Lin, Y.B., Lai, J.S., Chang, K.C., Chang, W.Y., Lee, F.Z. and Tan, Y.C. (2010). "Using mems sensors in the bridge scour monitoring system", *Journal of the Chinese Institute of Engineers*, 33(1), 25-35.

Melville, B.W. (1992). "Local scour at bridge abutments", *Journal of hydraulic engineering*, 118(4), 615-631.

Merlat, L. and Naz, P. (2003). "Magnetic localization and identification of vehicles", *Unattended Ground Sensor Technologies and Applications, SPIE*, 525-530.

Nagagawa, H. and Suzuki, K. (1975). "An application of stochastic model of sediment motion to local scour around a bridge pier", *Proceeding 16th International Association for Hydraulic Research Congress*, Sao Paulo, Brazil, 27 July-1 Aug, 2, 228-235.

Ren, H.L. and Hua, W. (2010). "Detection and localization of improvised explosive devices based on 3-axis magnetic sensor array system", *Symposium on Security Detection and Information Processing*, 1-9.

Shen, H.W., Schneider, V.W. and Karaki, S.S. (1969). "Local scour around bridge piers", *Journal of the Hydraulics Division*, 95(6), 1919-1940.

Shirole, A.M. and Holt, R.C. (1991). "Planning for a comprehensive bridge safety assurance program", *Journal of the Transportation Research Board*, 1290, 39-50.

Subhasish, D. and Rajkumar, V.R. (2007). "Characteristics of horseshoe vortex in developing scour holes at piers", *Journal of hydraulic engineering*, 133(4), 399-413.

Valentin. L.P. (2011). *Contact Mechanics and Friction: Physical Principles and Applications*, Beijing: Tsinghua university press.

Wynn, W.M. (1995). "Magnetic dipole localization using the gradient rate tensor measured by a five-axis magnetic gradiometer with known velocity", *Detection Technologies for Mines and Minelike Targets, SPIE*, 2496, 357-367.

Yu, X.B. and Yu, X. (2011). "Assessment of an Automation Algorithm for TDR Bridge Scour Monitoring System", *Advances in Structural Engineering*, 14(1), 13-24.

Zhang, L. and Xu, X. (2011). "Scour of the outfall and protection stones stability of houshi power plant", *Hydro-Science and Engineering*, 2, 14-19 (in Chinese).

Zhou, Y.L. and Cui, H.C. (1999). "Experiment research on the apron of bridge pier against the local scour", *Journal of Xi'an Highway University*, 19(3), 36-38 (in Chinese).

Zhou, Z., Huang, M.H., Huang, L.Q., Ou, J.P. and Chen, G.D. (2011). "An optical fiber bragg grating sensing

system for scour monitoring", *Advances in Structural Engineering*, 14(1), 67-78.